Journal of the Serbian Society for Computational Mechanics / Vol. 16 / No. 1, 2022 / pp 43-53
(10.24874/jsscm.2022.16.01.04)

A SUPERIMPOSED VALVELESS MICROPUMP USING NEW CHANNELS FOR OPTIMAL DRUG DELIVERY

Ahmed Slami*, Sofiane Soulimane

Department of Biomedical Engineering, Faculty of Technology, University of Tlemcen, 13000, Algeria
e-mail: ahmed.slami@univ-tlemcen.dz
e-mail: sofiane.soulimane@univ-tlemcen.dz
**corresponding author*

Abstract

In this paper, we propose a valveless micropump with an improved inlet/outlet channel configuration for biomedical applications. To do so, we added curved parts known as "ears" to a standard diffuser/nozzle shape. This new design will enlarge the flow rate values between both directions for the purpose of improving the valveless micropump efficiency. After that, the new channel is incorporated into a double valveless micropump superimposed on each other making the diaphragm in sandwich. This kind of micropump shows no reflux at its common outlet and good reliability due to the new design of the diffuser/nozzle channel. COMSOL Multiphysics software is used to model and simulate, under Fluid-Structure Interaction (FSI) physic, the complete system of the superimposed valveless micropump (SVM). The results are promising and show that our kind of micropump is necessary for medication injection because of the no backflow at its common outlet, and also because of the increase in its efficiency.

Keywords: valveless micropump, flow rate, drug delivery, FSI simulation, microfluidic channels, COMSOL Multiphysics.

1. Introduction

Diabetes is a widespread illness that affects a large number of people around the world. One of the harmful effects of hyperglycemia is that it weakens the entire body, and the patient will be unable to inject the medicine manually. As a result, micropumps are being developed to give insulin to patients automatically and safely. In addition, they are one of the wide applications of microfluidic devices in the biomedical field devices that have attracted a lot of attention because of their important role in drug administration, especially for insulin (Chappel & Dumont-Fillon, 2021). A pumping chamber with an inlet and outlet, a diaphragm, and an actuator are the main components of micropumps (Fig. 1). The actuator deforms the diaphragm inwards and outwards the pumping chamber by applying a mechanical force on it, on a regular basis. As a result, we can perceive the liquid suction and discharge from the inlet/outlet channels.

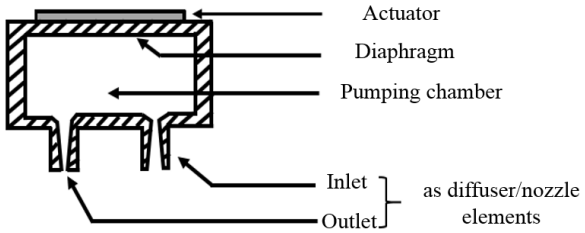

Fig. 1. Valveless micropump conception.

Several micropumps based on various principles and actuation techniques have been developed in recent years. Electromagnetic, piezoelectric, thermopneumatic, electrostatic, and others are examples of broad actuation systems. In comparison to other actuations, it is noted that the piezoelectrically one offers high accuracy and moderate pressure at low power consumption, making it excellent for medical applications (Cui, Liu, & Zha, 2008). In addition, the design of the micropump body plays an important role on its lifetime and efficiency as well as the choice of membrane's material and the structure of inlet/outlet channels. Micropumps are known as valveless and with valves opening channels. Those that include valves (Kang & Auner, 2011; Meshkinfam & Rizvi, 2015; Sim, Yoon, Jeong, & Yang, 2003; Wego & Pagel, 2001; Zengerle, Ulrich, Kluge, Richter, & Richter, 1995) are the most reliable in terms of flow rate because of their ability to completely open or close the channels. However, these kinds of channels break due to their reciprocating movement, which makes them weak and therefore unsuitable. As a result, there is a lot of interest in micropumps without valves (Choi, Vatanabe, de Lima, & Silva, 2012; Gamboa, Morris, & Forster, 2005; Morris & Forster, 2003; Singh, Kumar, George, & Sen, 2015; Stemme & Stemme, 1993; Tsai & Lin, n.d.) that do not present any moving parts, which makes them have a longer service life but with lower flow rates.

The diffuser/nozzle elements are frequently utilized structures in valveless micropumps (Chandrasekaran & Packirisamy, 2011; He, Zhu, Zhang, Xu, & Yang, 2017; Xu, Yan, Qin, & Cao, 2019; Yang, Chao, Chen, Wang, & Shyu, 2012) that replace valves and rectify fluid flow in one direction only. In other words, the flow rate depends on the direction of the fluid flow through the diffuser/nozzle, which is not the same for both directions (flow rate in diffuser direction is higher than in nozzle direction). While such features extend the lifetime of these biomedical micropumps, it is necessary to increase their efficiency by enlarging the difference in flow rates between the diffuser and nozzle directions.

Our main goal in this present work is to enhance the diffuser/nozzle reliability, which will increase the micropump efficiency. Therefore, the structure of the conventional diffuser/nozzle is tuned so as to ensure the decreasing of flow rate in nozzle direction as much as possible. So, we added and adjusted a two-ear design to the sides of the conventional structure of the diffuser/nozzle element. This tuning is conducted in such a manner not to influence the flow rate in the diffuser direction. After that, we placed a second micropump on top of the first one, creating a sandwich diaphragm that could be utilized at the same time for both of micropumps. This configuration eliminates by hundred percent the fluid backflow which makes this micropump very useful for drug injection without any risk possible.

This paper starts by introducing the different micropumps used in the biomedical field. After that, the important parameters and micropump principle of functions are described in detail. In addition, the method of modeling and simulation using COMSOL Multiphysics is presented. Finally, the results of the simulation are shown and discussed.

2. Method

2.1 Diffuser/Nozzle element

The most used geometry in microfluidic systems that makes the flow rate depending on the flow direction through is the diffuser/nozzle element. This behavior is similar to that of an electrical diode, but with some leak.

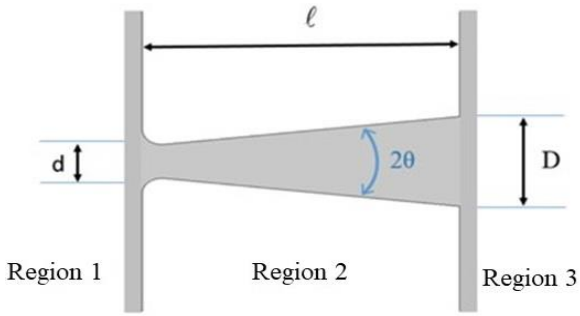

Fig. 2. Schema of the diffuser/nozzle element.

As depicted in Fig. 2, three regions are important for describing fluid flow characteristics: The first region is a small area with an opening 'd' , called "throat". It is the narrowest part of the diffuser/nozzle. The second region is a narrowing/widening channel with a length 'l' and an opening angle of '2θ' . The third region is a large area with an opening 'D' . The principle of function of the diffuser/nozzle element is based on the pressure losses of the fluid in these regions, depending on the direction of flow. When the flow goes from the small to the wide opening (through the widening direction), the structure is called a diffuser. In the narrowing direction, it is called a nozzle.

The global pressure losses into the Diffuser/Nozzle element are given in equations (1) and (2) (Stemme & Stemme, 1993) :

$$\Delta P_{Diff} = \frac{1}{2}\rho V^2 K_{Diff} \tag{1}$$

$$\Delta P_{Nozz} = \frac{1}{2}\rho V^2 K_{Nozz} \tag{2}$$

where ΔP_{Diff} and ΔP_{Nozz} are the global pressure losses in diffuser and nozzle respectively; ρ ρ is the fluid density and V is the fluid velocity in the throat. K_{Diff} and K_{Nozz} are the coefficients of the global pressure loss in diffuser and nozzle directions respectively. The fluidic diode effect of the diffuser/nozzle element is due to that K_{Diff} is lower than K_{Nozz} .

The flow rates in the diffuser Q_{Diff} and in the nozzle Q_{Nozz} are calculated using the equations (3) and (4):

$$Q_{Diff} = V_{Diff} * S_T \tag{3}$$

$$Q_{Nozz} = V_{Nozz} * S_T \tag{4}$$

where S_T is the area of the throat.

In this paper, the efficiency of a diffuser/nozzle element is evaluated through the value of the net flow rate Q_{net}, given by the equation (5):

$$Q_{net} = Q_{Diff} - Q_{Nozz} \tag{5}$$

2.2 Valveless micropump

The difference in pressure losses is then used to operate a valveless micropump. For a complete pumping cycle, Fig. 3 depicts the basic characteristics of fluid flow into the inlet/outlet channels.

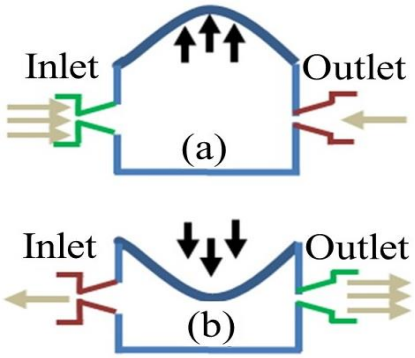

Fig. 3. Pumping cycle of valveless micropump. (a) Suction mode; (b) Pump mode.

In the suction mode, the membrane bends outward, resulting in a higher differential pressure at the inlet than at the outlet (Fig. 3a). As a result, the entrance receives more liquid than the outlet. Second, in pumping mode, the membrane bends inward, resulting in a lower differential pressure at the inlet than at the outlet (Fig. 3b). Therefore, more liquid escapes the outlet than it enters the inlet.

As can be seen at the micropump outlet (Fig. 3), from where the medicine is provided to the patient, the fluid makes an out-and-back motion. This will cause a little amount of blood aspiration from the patient, which is completely unacceptable. For this reason, a second micropump is called and applied to the first one in some configuration that helps in elimination of backflow at the outlet. Fig. 4 shows the complete pumping cycle for the SVM using only one diaphragm in sandwich between two pumping chambers, and four diffuser/nozzle elements connected to two common inlet/outlet channels.

In the first half cycle of pumping, the membrane bends upwards, causing the first micropump to function as in suction mode while the second micropump works as in pumping mode (Fig. 4a). As a result, the SVM will aspire the liquid from the common inlet, due to the higher incoming fluid flow rate of the first micropump (Ch1) than the outgoing fluid flow rate of the second one (Ch2). Thus, the inlet flow rate is the sum of the two flow rates of the incoming and the outgoing fluid flow rates of the first and the second micropumps respectively. On the other hand, the SVM will pump the liquid through the common outlet, due to the higher outgoing fluid flow rate of the second micropump (Ch2) than the incoming fluid flow rate of the first one (Ch1). Hence, the outlet flow rate is the sum of the two flow rates of the outgoing and the incoming fluid flow rates of the second and the first micropumps respectively.

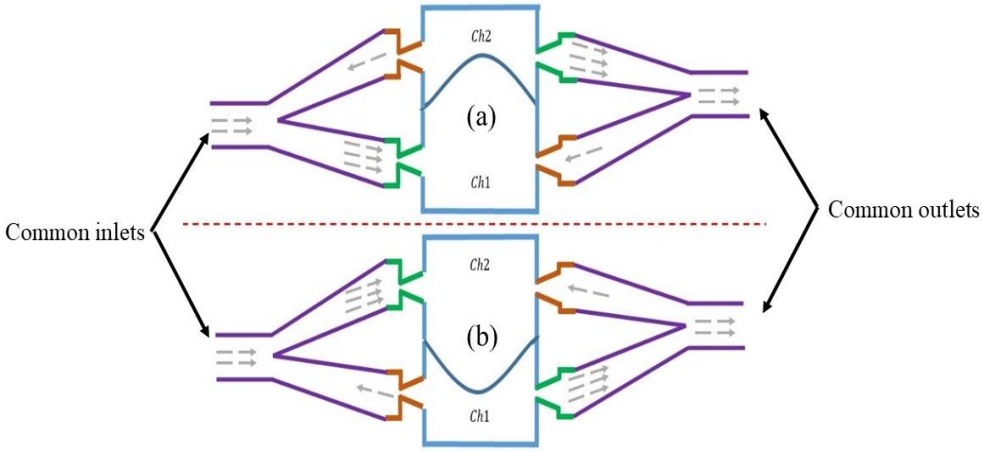

Fig. 4. Pumping cycle of the SVM. (a) Suction mode; (b) Pump mode.

In the second half cycle of pumping, the diaphragm bends downwards, making the first micropump function as in pumping mode whereas the second operates as in suction mode (Fig. 4b). Despite the two micropumps' roles being reversed, it did not prevent the SVM from working as well as in the first pumping half cycle. As a result, for the full pumping cycle of the SVM, it works only in the way that the fluid is always supplied through the common inlet and pumped from the common outlet. Therefore, it is highly suitable to be used for injecting medications because of there is no backflow. Although this SVM is the best choice for drug delivery, it is encouraged to improve its reliability to make it more optimal.

2.3 Diffuser/nozzle element with a two-ear design

Fig. 5 shows the new structure of the diffuser/nozzle channels for valveless micropump where we fitted and adapted on their sidewalls a two-ear design. The benefit of this new design is that it will not affect the flow rate in the diffuser direction (Fig. 5a), but in the nozzle direction (Fig. 5b) it will decelerate the flow rate so as to enlarge the difference in the flow rate of both directions (forward and backward), and then the efficiency is enhanced.

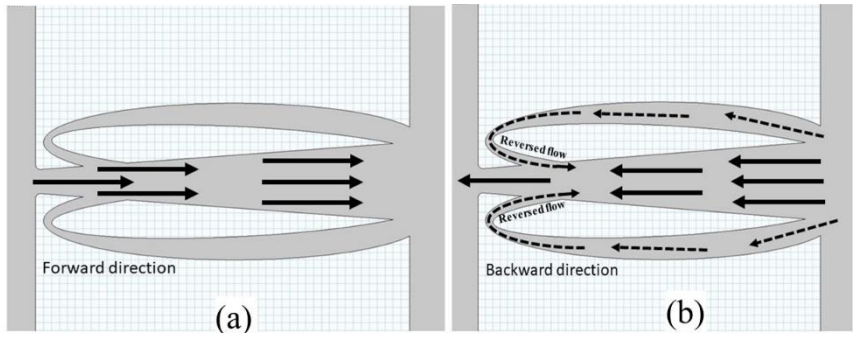

Fig. 5. Working principle of the new diffuser/nozzle structure. (a) Forward direction; (b) Backward direction.

2.4 Method of simulation

In this study, the different characteristics of the valveless micropump are carried out using the COMSOL Multiphysics software 5.5, which is based on the finite element model. Under the computer aided design (CAD) of the COMSOL software and, following the schema presented in Fig. 4, we start by modeling in 3D domain our new structure of the SVM (Fig. 6) and all its parts (membrane, chambers, diffuser/nozzle channels, common inlet/outlet, etc.). In order to lessen the calculation time, the external body of the SVM is not affected. After that, the PolyDiMethylSiloxane (PDMS) is attributed to the membrane while water is attributed to the rest of the structure.

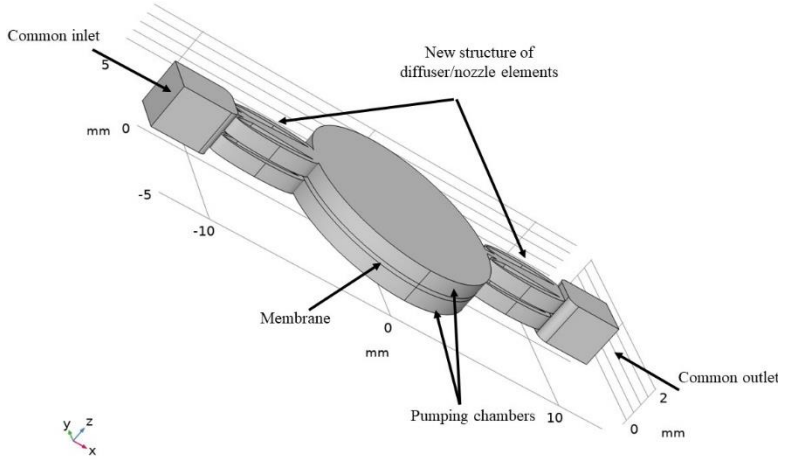

Fig. 6. 3D model of the SVM conception.

The Fluid-Structure Interaction (FSI) physic is called to strongly couple between the fluid flow and the solid mechanics analyses. In order to combine solid mechanics that are described using a Lagrangian description and a material (reference) frame with fluid flow that is described using a Eulerian description and a spatial frame, the FSI interface uses an implicit scheme for the arbitrary Lagrangian-Eulerian (ALE) technique. For the fluid flow analysis and, as long as the Reynolds number is below a critical value of approximately 2000 and the fluid is considered incompressible, laminar fluid interface is used to solve Navier-Stokes equations which include the momentum and continuity equations as follows,

$$\rho(\frac{\partial}{\partial t}u_{fluid}.\nabla)u_{fluid} = -\nabla p + \mu\nabla^2 u_{fluid} \tag{6}$$

$$\rho\nabla.u_{fluid} = 0 \tag{7}$$

where ρ is the fluid density, u_{fluid} is the fluid velocity, p is the pressure and, μ is the dynamic viscosity.

Then, for the solid mechanic interface which study the deformation and motion of the SVM membrane under the action of forces, the governing equation for the membrane deflection (while considered a linear elastic material) is given by:

$$\rho\frac{\partial^2}{\partial t^2}u_{solid} = \nabla.(FS)^T + F \tag{8}$$

where u_{solid} is the solid displacement, S is the second Piola-Kirchhoff stress tensor and, F is the strain-displacement tensor given by,

$$F = \nabla . u_{solid} + I \tag{9}$$

It is noted that the displacements of the solid domain cause a mesh deformation in the spatial frame. So, within the fluid domains, the mesh is extended in its mobility and reacts to the motion of the solid walls. The ALE approach in COMSOL software automatically takes into consideration the moving mesh to combine the structural and fluidic domains motions.

Finally, an auto-mesh is generated in order to determine the meshing sequence according to the coupling between fluid dynamics and solid mechanics. As a result, the number of the mesh elements for the whole SVM with the new design of the diffuser/nozzle channels is 611406 elements, which is higher than that with standard diffuser/nozzle channels: 377163 elements.

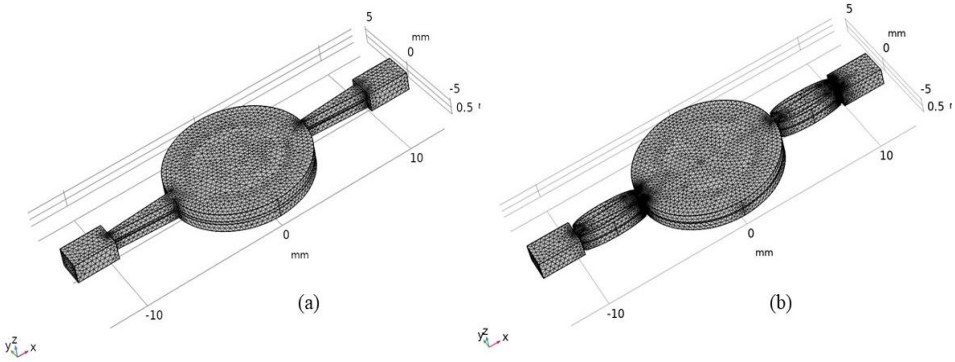

Fig. 7. Meshing of the SVM. (a) Conventional channels; (b) Enhanced channels.

3. Results and discussions

All simulations are using the time-dependent study in a range of 0.25 seconds with a step of 0.001 sec. An oscillating force is applied on the SVM diaphragm along the Z-axis using the equation below:

$$Frc(t) = Frc.\sin(2\pi ft) \tag{10}$$

where Frc is the applied force amplitude.

It is important to note that to reduce the computational time, which is related to the meshing elements number, different parameters are tuned on the SVM with the conventional diffuser/nozzle channels (Fig. 8 and Fig. 9) in order to make it as reliable as possible. After that, the best configuration obtained is used to simulate the SVM with the enhanced diffuser/nozzle channels (Fig. 10, Fig. 11, and Fig. 12). The simulations were run on a computer with an AMD Ryzen threadripper CPU with 64 Go of random memory, and each simulation took around 5 hours of calculation. Also, the results of the micropump flow rate and the pumped volume are always taken from the common outlet (Fig. 6).

Fig. 8 presents the variation of the flow rate versus different membrane thickness while applying the same oscillating force of Frc=0.12N. As we can see, the difference in flow rate variations for different thicknesses of the membrane is negligible because of the PDMS capability to easily deform under weak forces.

Fig. 9 shows maximum displacement variation of the membrane, the flow rate, and the pumped liquid versus applied different oscillating forces with Frc: 0.10N, 0.13N, 0.15N, 0.17N, and 0.19N. The maximum displacement (Fig. 10a) obtained was for Frc=0.19N which makes the membrane deform until the depth of the pumping chamber (0.5mm). The flow rate variation (Fig. 10b) shows a maximum of approximately 2.8 ml/min and the mean of the pumped liquid (Fig. 10c) is for 30µl per minute.

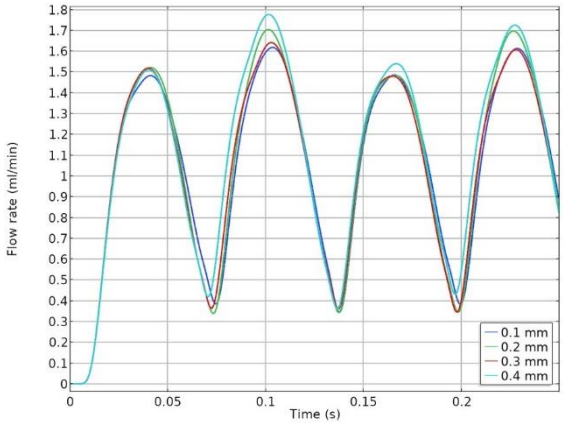

Fig. 8. Flow rate variation versus different membrane thickness.

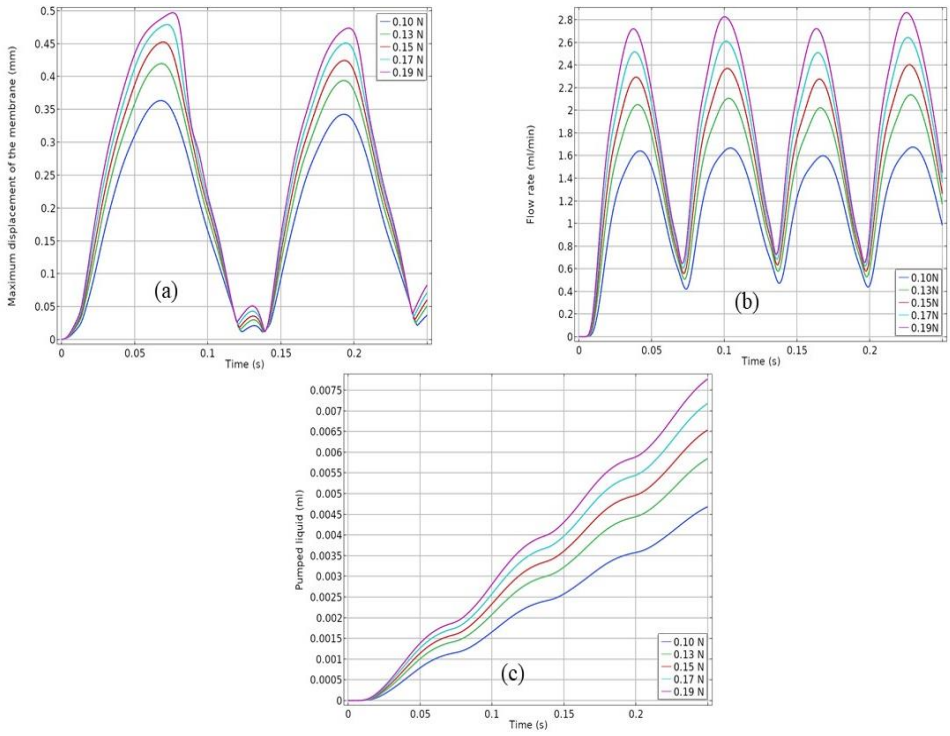

Fig. 9. Maximum membrane displacement (a), flow rate variation (b), pumped liquid (c) versus applied different oscillating forces.

Once the different parameters of the SVM with conventional diffuser/nozzle channels are now the most optimized, the new design of the diffuser/nozzle channels is then implemented.

Fig. 10 is extracted to illustrate the distribution of the fluid velocity through just one micropump of the SVM (the bottom one) using a cut plane (XY) at Z=0.25mm when the flow rate is higher. It is clear that in the latter the fluid does not enter through both channels with the same velocity. The fluid velocity in the left channel is higher than the right one. Fig. 11 shows clearly this special effect of the new design that does not disturb the fluid flow in the diffuser direction (Fig. 11a) while in the nozzle direction (Fig. 11b) the fluid flow is decelerated because of the reversed flow attacking the main fluid flow (zoomed area in Fig. 11b). As a result, the flow rate is enlarged between both directions. It's important to note that in just one micropump, the reflux of the liquid is present, which is the goal of using a SVM (Fig. 4).

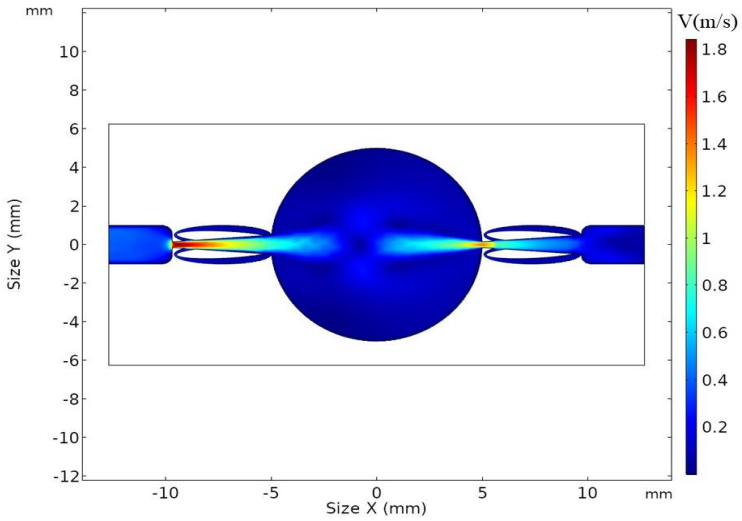

Fig. 10. Distribution of the fluid velocity through just one micropump of the SVM while the flow rate is higher (6ml/min).

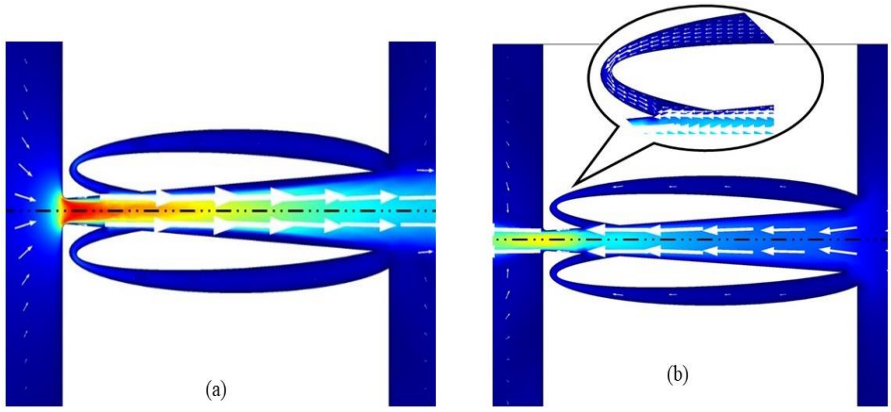

Fig. 11. Distribution of the fluid velocity through the new design of the diffuser/nozzle channels into the micropump mentioned in Fig.10. (a) diffuser direction (b) nozzle direction.

Fig. 12 depicts the variation of maximum displacement of the SVM membrane (Fig. 12a), the flow rate (Fig. 12b), and the pumped liquid (Fig. 12c) in comparison between the SVM using standard diffuser/nozzle channels (solid line) with that using the new design of the diffuser/nozzle channels (dashed line). The new one performs better despite employing the same force (0.19N) that can be seen on the diaphragm maximum displacement. The flow rate variation reaches a maximum of around 6 ml/min, and the pumped liquid average is 72 µl per minute.

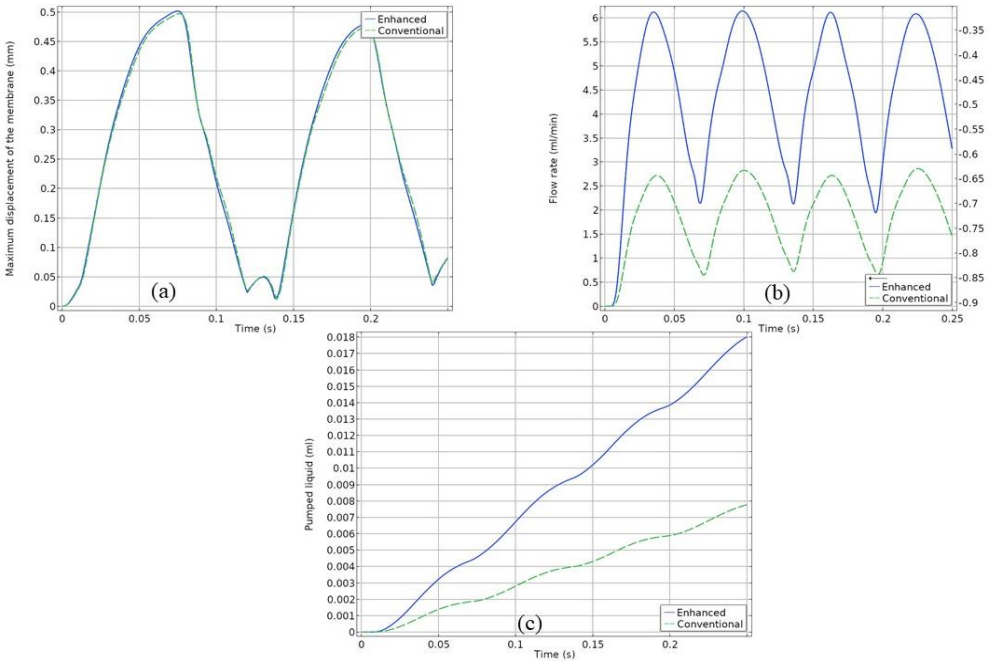

Fig. 12. Comparison study of the maximum membrane displacement (a), flow rate variation (b), pumped liquid (c).

It is noted in all figures of flow rate variations (Fig. 8, Fig. 9b, and Fig. 12b) that there are no minus values, which means there is no reflux of the pumped liquid in the SVM common outlet.

4. Conclusions

In this paper, a superimposed valveless micropump with a new design of the diffuser/nozzle channels is modeled and simulated using COMSOL Multiphysics software. The main goal of this work is, on the one hand, to improve the reliability of the valveless micropump and, on the other hand, to make it ideal for drug delivery without any risk of reflux. Therefore, two micropumps are superimposed on each other making only one membrane in sandwich. In addition, a new design of diffuser/nozzle channels is utilized by adding a two-ear structure to the conventional diffuser/nozzle. This new architecture shows very promising results in terms of reliability (up to 214%). These results show that the SVM with the new design of channels is very optimal, reliable and, suitable for medication delivery because there is no backflow.

Acknowledgements The authors thank the Directorate-General of Scientific Research and Technological Development (DGRSDT) for financial assistance towards this research, URL: www.dgrsdt.dz, Algeria.

References

Chandrasekaran A, and Packirisamy M (2011). Geometrical tuning of microdiffuser/nozzle for valveless micropumps. *Journal of Micromechanics and Microengineering*, *21*, 045035.

Chappel E and Dumont-Fillon D (2021). Micropumps for drug delivery. In *Drug Delivery Devices and Therapeutic Systems* (pp. 31–61). Elsevier.

Choi A, Vatanabe S L, de Lima, CR, Silva ECN (2012). Computational and experimental characterization of a low-cost piezoelectric valveless diaphragm pump. *Journal of Intelligent Material Systems and Structures*, *23*, 53–63.

Cui Q, Liu C, and Zha XF. (2008). Simulation and optimization of a piezoelectric micropump for medical applications. *The International Journal of Advanced Manufacturing Technology*, *36*, 516–524.

Gamboa AR, Morris CJ, Forster FK (2005). Improvements in Fixed-Valve Micropump Performance Through Shape Optimization of Valves. *Journal of Fluids Engineering*, *127*, 339–346.

He X, Zhu J, Zhang X, Xu L, Yang S (2017). The analysis of internal transient flow and the performance of valveless piezoelectric micropumps with planar diffuser/nozzles elements. *Microsystem Technologies*, *23*, 23–37.

Kang J and Auner GW (2011). Simulation and verification of a piezoelectrically actuated diaphragm for check valve micropump design. *Sensors and Actuators A: Physical*, *167*, 512–516.

Meshkinfam F and Rizvi G (2015). *Design and Simulation of MEMS Based Piezoelectric Insulin Micro- Pump*. 6.

Morris CJ and Forste FK (2003). Low-order modeling of resonance for fixed-valve micropumps based on first principles. *Journal of Microelectromechanical Systems*, *12*, 325–334.

Sim WY, Yoon HJ, Jeong OC, Yang SS (2003). A phase-change type micropump with aluminum flap valves. *Journal of Micromechanics and Microengineering*, *13*, 286–294.

Singh S, Kumar N, George D, Sen AK (2015). Analytical modeling, simulations and experimental studies of a PZT actuated planar valveless PDMS micropump. *Sensors and Actuators A: Physical*, *225*, 81–94.

Stemme E and Stemme G (1993). A valveless diffuser/nozzle-based fluid pump. *Sensors and Actuators A: Physical*, *39*, 159–167.

Tsai J-H and Lin L (n.d.). *A Thermal Bubble Actuated Micro Nozzle-Diffuser Pump*. 4.

Wego A and Pagel L (2001). *A self-®lling micropump based on PCB technology*. 7.

Xu Y, Yan W, Qin K and Cao T (2019). Three-dimensional flow field simulation of steady flow in the serrated diffusers and nozzles of valveless micro-pumps. *Journal of Hydrodynamics*, *31*, 413–420.

Yang K-S, Chao T-F, Chen IY, Wang CC, Shyu J-C (2012). A Comparative Study of Nozzle/Diffuser Micropumps with Novel Valves. *Molecules*, *17*, 2178–2187.

Zengerle R, Ulrich J, Kluge S, Richter M, Richter A (1995). A bidirectional silicon micropump. *Sensors and Actuators A: Physical*, *50*, 81–86.